Dopamine-induced dissociation of BOLD- and neural activity in macaque visual cortex

Daniel Zaldivar[1,2], Alexander Rauch[1,3], Kevin Whittingstall[4], Nikos K. Logothetis[1,5], Jozien Goense[1,6]

[1] Max Planck Institute for Biological Cybernetics; Spemannstrasse 38, D-72076 Tübingen, Germany.
[2] IMPRS for Cognitive and Systems Neuroscience, University of Tübingen; Österbergstrasse 3, D-72074 Tübingen, Germany
[3] University Hospital of Psychiatry, University of Bern CH-3000, Bern, Switzerland.
[4] Département de Radiologie Diagnostique 3001, Université de Sherbrooke, 12e Avenue Nord Sherbrooke J1H 5N4, Québec, Canada
[5] Division of Imaging Science and Biomedical Engineering, University of Manchester; Manchester M13 9PT, United Kingdom
[6] Institute of Neuroscience and Psychology, University of Glasgow; 58 Hillhead Street, Glasgow G12 8QB, United Kingdom

RUNNING TITLE

BOLD and neuronal dissociation induced by dopamine

SUMMARY

Neuromodulators determine how neural circuits process information during cognitive states such as wakefulness, attention, learning and memory **[1]**. fMRI can provide insight into their function and dynamics, but their exact effect on BOLD-responses remains unclear **[2-4]**, limiting our ability to interpret the effects of changes in behavioral state using fMRI. Here, we investigated the effects of dopamine (DA) injections on neural- and haemodynamic signals in macaque V1 using fMRI (7T) and intracortical electrophysiology. Aside from dopamine's involvement in diseases such as Parkinson's and schizophrenia, it also plays a role in visual perception **[5-8]**. We mimicked DAergic neuromodulation by systemic injection of L-DOPA+Carbidopa (LDC) or by local application of DA in V1 and found that systemic application of LDC increased the signal-to-noise ratio (SNR) and amplitude of the visually

evoked neural responses in V1. However, visually induced BOLD-responses decreased, while cerebral blood flow (CBF)-responses increased. This dissociation of BOLD and CBF suggests that dopamine increases energy metabolism by a disproportionate amount relative to the CBF-response, causing the reduced BOLD-response. Local application of DA in V1 had no effect on neural activity, suggesting the dopaminergic effects are mediated by long-range interactions. The combination of BOLD- and CBF-based fMRI can provide a signature of dopaminergic neuromodulation, indicating the application of multimodal methods can improve our ability to distinguish sensory processing from neuromodulatory effects.

RESULTS

We combined fMRI with neurophysiology and pharmacology in five anesthetized non-human primates (*Macaca mulatta*), where we acquired BOLD, functional CBF (fCBF) and electrophysiology data while the animals viewed a rotating checkerboard stimulus. Figure 1A shows the experimental paradigm. We pharmacologically mimicked DAergic neurotransmission by systemic application of L-DOPA and Carbidopa. Carbidopa inhibits the breakdown of L-DOPA in the periphery, thereby preventing systemic changes in cerebral blood volume (CBV) that may affect the fMRI results (Figure S1). The lack of systemic effects of the LDC injection is evidenced by the highly stable physiological parameters during and after injection (Table S1).

Evoked BOLD and neural responses under systemic LDC

Figure 1B shows representative fMRI responses in V1 to visual stimulation. Figure 1C shows the changes in the BOLD-response over the course of the LDC injection. BOLD-modulation in the pre-drug period was 2.5±1.1%, which is typical for anesthetized monkeys at 7T **[9-11]**. During the drug infusion we observed a significant reduction in the visually induced modulation (Figure 1C,D; MOD_{drug}=50±5.3%; p=0.034), which was sustained after the infusion was stopped (MOD_{post}=60±4.2%; p=0.05). No significant changes in the baseline were found (Figure 1D).

We recorded local field potentials (LFP) and multiunit spiking activity (MUA) to evaluate the effects of LDC application on neural activity. The power in three different frequency ranges was calculated: γ (40-150 Hz) and MUA (900-3000 Hz), which are most strongly correlated with the BOLD signal **[2, 3, 12]**, while θ (4-8 Hz) was used to indicate whether LDC affects the broadband-LFP power and to assess whether DA-injection induces changes in the level of anesthesia. Figure 2A-C shows the average time course across experiments for the θ-, γ- and MUA-bands respectively. LDC application resulted in an 18% increase in visual modulation in the γ-band (Figure 2D; $MOD_{\gamma,drug}$=118±4.2%; p=0.024) and a 19% increase in the MUA-band ($MOD_{MUA,drug}$=119±5%; p=0.031). The effect of LDC on the MUA-amplitude

reached baseline values ~4.5 min after the infusion was stopped. In contrast, for the γ-band the increase in visually induced modulation was long-lasting and started to reduce ~12 min after the infusion was stopped. Additionally, we observed an increase in the SNR of the γ- and MUA-bands starting shortly after LDC injection (Figure 2E); the response to the stimulus increased while the variability decreased (Figure 2B,C). The SNR in the γ-band ($SNR_{\gamma,drug}$=13.7±2.0 dB; p=0.011) kept increasing after the infusion was stopped ($SNR_{\gamma,post}$=14.7±2.0 dB; p=0.012). The MUA-band also showed an SNR-increase after the start of the injection ($SNR_{MUA,drug}$=12.2±2.2 dB; p=0.012) which continued until the end of the trial ($SNR_{MUA,post}$=11.0±2.0 dB; p=0.026). In the θ-band (Figure 2A) neither visually induced modulation nor SNR changed upon LDC infusion.

Dopamine effects are not locally induced in V1

We next investigated whether the increases in neural activity are locally induced in V1 or are due to a remote influence from other regions by injecting DA intracortically in V1 to determine whether this induces similar effects as systemic dopamine. Figure 3A-C shows the averaged traces of the θ-, γ- and MUA-bands during intracortical application of DA (5 mM) and shows no discernible changes. Visually induced modulation in the γ- and MUA-bands (Figure 3D) was unchanged (p=0.23). The SNR of the γ- and MUA-bands also remained unchanged during the experimental session (Figure 3E, $SNR_{\gamma,drug}$=9.0±1.5 dB; p=0.31; $SNR_{\gamma,post}$=8.8±2.0 dB; p=0.13; $SNR_{MUA,drug}$=10.1±0.5 dB; p=0.18; $SNR_{MUA,post}$=10.8±2.0 dB; p=0.18). Since different concentrations of DA can exert multiple modes of action **[13]**, we tested whether different concentrations of intracortical DA affected the responses in V1. However, no concentration dependent effects were observed (Figure S2).

The effects of LDC on CBF suggest an increase in energy expenditure

Stimulus-induced increases in γ-power and in MUA occurred simultaneously with a decrease in BOLD-modulation. To resolve this potential discrepancy we measured fCBF using arterial-

spin-labeling (ASL). Figure 4A shows fCBF in early visual cortex and Figure 4B the averaged time course of the CBF across experiments. There was a reliable visually induced, CBF-modulation of 19±7% during the pre-drug period, in agreement with earlier studies **[11]**. During the 'drug' period we observed an increase in modulation by 34% (MOD_{drug}=134±10%; p=0.045). The maximum CBF-increase of 43% was observed ~12 min after the infusion started and lasted ~20 min (MOD_{post}=143±10%; p=0.034). We also observed significant increases in baseline CBF during and after the injection. An increase in the baseline was evident ~8 min after the start of the injection ($CBF_{baseline,drug}$=128±5.2%; p=0.022). The time course of the CBF-changes upon LDC injection were similar to the time courses of the changes in the neuronal responses, suggesting that increases in neural activity may cause the CBF-increases.

DISCUSSION

Using BOLD- and CBF-based fMRI combined with intracortical electrophysiology, we found that DAergic neuromodulation increased neural- and CBF-responses to a visual stimulus, while decreasing the BOLD-response. Neuromodulators can exert strong influences on neural responses and alter neurovascular coupling **[1, 3]**; our results show that changes in the BOLD-fMRI signal alone cannot be used to make inferences about increases or decreases in the underlying neural activity.

Neurophysiological effects of dopamine injection

Neurophysiological recordings under systemic LDC injection showed an increase in the amplitude and SNR of visually evoked responses. DA has been shown to improve the SNR in PFC and in sensory areas, including V1 **[8, 14-16]**, thereby changing detection performance at the behavioural level **[8, 16-18]**. Increased neuronal activity in V1 has been shown to predict the timing of reward delivery, even when the cells were not driven by a visual stimulus **[8, 18]**, highlighting the importance of DA for extracting behaviourally relevant information **[17, 19]**.

However, local dopamine application did not change neural activity, in good agreement with the low density and sparse distribution of DARs in V1 **[20]** and suggesting that DA does not exert its effects on V1 itself. The increase in neural activity upon systemic DA may be mediated by long-range interactions from higher-order regions, for instance frontal regions **[5, 15]**. Large-scale interactions have been reported in other sensory modalities, including the visual-, somatosensory- and auditory systems, suggesting that DA prepares the higher-order area for the processing of incoming sensory signals, and promotes the readout of task-related information **[14-16]**. Manipulation of prefrontal D1-receptors increased the magnitude, reliability and selectivity of neuronal responses in V4 **[5]**, and similar mechanisms may play a role in V1.

The lack of DAergic effects upon local application is contrary to the inhibitory responses observed earlier **[21, 22]**. Although DA can exert different actions depending on concentration **[13]**, none of the DA concentrations used in this study changed the amplitude or SNR of the visually evoked responses. Aside from species differences **[20, 23]**, another possibility that could explain the differences is that the earlier experiments were performed with solutions in which the pH was not tightly controlled, whereas acidic pH depresses neuronal excitability **[24]**.

Functional imaging

Our finding of a decrease in the evoked BOLD-response and an increase in the CBF-response upon systemic LDC injection, extends previous observations in humans and macaques in which fMRI responses in V1 decreased with cues that predict and anticipate reward **[6, 19]**. A decrease in BOLD-responses in V1 while behavioral performance improved after an acute dose of L-DOPA was seen in studies of amblyopia **[7, 25]**. However, BOLD-increases have also been observed in humans in primary auditory and somatosensory cortex after DA-agonist administration **[26, 27]**. These differences in BOLD-responses upon DAergic neuromodulation can be partly explained by the difference in densities of DARs and DA-innervation between cortical regions. DARs and DA-innervations

decrease along a rostro-caudal gradient having the highest density in PFC and the lowest (or almost nonexistent) in occipital cortex **[20]**. Thus, BOLD-responses to DAergic neuromodulation could differ in various sensory cortices, since local influences of DA on the vasculature may modulate the blood supply **[28, 29]**.

The effects of DA on the hemodynamic signals have been extensively addressed using different pharmacological agents in rats and monkeys **[29-33]**. For instance, amphetamines decreased CBV-responses in occipital regions **[33]**. However, amphetamines are known to increase DA-levels as well as alter the kinetics of other neurochemicals that affect the regional CBV **[34]**, while CBV-responses may differ from BOLD-responses **[35]**. Different DARs exert different effects on the hemodynamic signals **[30]**; stimulation of D1-receptors (D1Rs) increases CBV and BOLD **[30, 32]** whereas blocking these receptors decreases it **[30, 36]**. The activation and deactivation of D2-receptors (D2Rs) produces opposite effects **[37]**. The present study did not consider receptor specific-responses, but instead focused on understanding the balanced effects mediated by D1R and D2R interaction.

Neurovascular coupling under dopamine

Changes in the LFP are usually mirrored by changes in spiking and in the haemodynamic responses **[12]**. Our observation of a dissociation between the BOLD- and neurophysiological responses indicates that neurovascular coupling may differ under states of neuromodulation. Our results suggest that the increase in neural activity and CBF and the decrease in BOLD are caused by a disproportionate increase in O_2-consumption due to DAergic neuromodulation. The BOLD-signal reflects the deoxyhemoglobin concentration [dHb], and is affected by CBF, CBV and the cerebral metabolic rate of oxygen consumption ($CMRO_2$). The stimulus-evoked BOLD-decrease could be due to a CBF-decrease or a [dHb] increase after dopamine application. Since CBF increased, dHb-production is most likely also increased, i.e. an increase in $CMRO_2$. An increase in CBF-modulation and a decrease in BOLD-response can occur when the O_2-consumption increases by a proportionally larger

amount than the inflow of fresh blood, leading to a relative increase in [dHb] and a decrease in the BOLD-signal compared to the pre-injection response.

The increased neural activity also suggests a $CMRO_2$-increase, since it has been shown that improving neurons' sensitivity is energetically draining **[17, 38]**. Using autoradiography it has also been shown that the application of L-DOPA increases brain metabolism **[39]**. These observations are not surprising given that energy usage is tightly coupled to neural performance **[3, 38]**. The increase in CBF likely relates to neuronal activity because glucose metabolism, $CMRO_2$ and CBF are closely coupled **[3, 40]**. Increased neural activity in response to reward increases has been shown to increase the CBF **[41]**.

The increased baseline CBF upon acute LDC injection commonly seen in humans and non-human primates **[42-44]** is usually attributed to vasodilation. However, the stimulus-induced CBF-increases cannot be attributed to vasodilation alone. Vasodilation increases the baseline CBF- and BOLD-signals, and reduces stimulus-evoked CBF- and BOLD-signals due to limited reserves, as seen in the case of hypercapnia (a potent vasodilator) **[45, 46]**. The possibility that the BOLD-reduction is due to a ceiling effect, as seen in the case of hypercapnia or in pathology, is therefore unlikely, since evoked CBF decreases in the case of vasodilation (e.g. in hypercapnia) or an inadequate CBF-response **[47]**.

PET-studies have shown little or no change in $CMRO_2$ upon L-DOPA administration **[43]**, the latter reflecting little or no change in baseline response, as was observed here. A lack of $CMRO_2$-increase however, would not be able to explain our stimulus-driven results: comparing again with hypercapnia where $CMRO_2$ and neural activity do not change considerably; this would lead to very different CBF- and BOLD-responses to the stimulus than observed here **[45]**. Whether the increase in baseline CBF corresponds to an increase in metabolism cannot be deduced based on the current data. The baseline of the BOLD time-course did not change, with a minor tendency to go down. It is possible that the increase in CBF is balanced out by an increase in [dHb] in the baseline state, leading to little or no net baseline changes. Following the same reasoning as with the stimulus-induced

responses, the small decrease in the baseline BOLD-trace may indicate a small increase in $CMRO_2$ in the baseline condition as well. However, further study is needed to verify this.

The effects observed here are unlikely to be due to DA-induced changes in the level of anaesthesia, since no differences were observed in the θ-band or the physiological parameters. The advantage of using anesthetized animals is that we could assess the effect of dopamine on neural and hemodynamic properties without needing to take behavioural parameters like attention, reward and anticipation into account. Anesthetized animals also allow us to discriminate small changes since it allows for longer averaging times. However, differences in regional CBF under DAergic influence have been observed between awake and anesthetized animals **[42]**, and differences may depend on the type anaesthesia. Since neuromodulatory properties strongly depend on the animal's behavioural state, including its level of alertness, this highlights the complexity of fMRI studies of neuromodulation, and ideal would be a comparison of dopaminergic effects in awake and anesthetized animals.

The findings presented here provide us with a better understanding of the influence of neuromodulation on fMRI-signals. The decrease of the BOLD-signal in the face of an increased energy use, implies that the BOLD-response may not always faithfully reflect the neural responses under neuromodulation, and imply caution is necessary in interpreting BOLD-signals under neuromodulation. Combining BOLD-measurements with CBF- and/or CBV-measurements can resolve these complexities and potentially provide a tool to discriminate sensory processing from neuromodulation. Such multidisciplinary approaches may improve the interpretation of fMRI-studies where neuromodulation plays a role, for example, studies of reward or attention, but also facilitate clinical applications of fMRI.

EXPERIMENTAL PROCEDURES

fMRI and electrophysiology data were collected from six (four females) healthy rhesus monkeys *(Macaca mulatta;* 5–11 kg, 6-12 years). All experimental procedures were carried out under approval of the local authorities (Regierungspräsidium, Baden-Württemberg, Tübingen, Germany, Project K4/09) and were in full compliance with the guidelines of the European Community (EUVD 86/609/EEC).

ACKNOWLEDGMENTS

We thank Thomas Steudel, Mirko Linding and Deniz Ipek for valuable technical support; Hellmut Merkle for designing and building the RF-coils. We thank Veronika von-Pfoestl and Cesare Magri for help with experiments. Raymundo Baez-Mendoza and Yusuke Murayama provided comments on an earlier version of the manuscript. This work was supported by the Max Planck Society.

REFERENCES

1. Dayan, P. (2012). Twenty-five lessons from computational neuromodulation. Neuron *76*, 240-256.
2. Rauch, A., Rainer, G., and Logothetis, N.K. (2008). The effect of a serotonin-induced dissociation between spiking and perisynaptic activity on BOLD functional MRI. PNAS *105*, 6759-6764.
3. Logothetis, N.K. (2008). What we can do and what we cannot do with fMRI. Nature *453*, 869-878.
4. Sirotin, Y.B., and Das, A. (2009). Anticipatory haemodynamic signals in sensory cortex not predicted by local neuronal activity. Nature *457*, 475-479.
5. Noudoost, B., and Moore, T. (2011). Control of visual cortical signals by prefrontal dopamine. Nature *474*, 372-375.
6. Arsenault, J.T., Nelissen, K., Jarraya, B., and Vanduffel, W. (2013). Dopaminergic reward signals selectively decrease FMRI activity in primate visual cortex. Neuron *77*, 1174-1186.
7. Rogers, G.L. (2003). Functional magnetic resonance imaging (fMRI) and effects of L-dopa on visual function in normal and amblyopic subjects. Trans Am Ophthalmol Soc *101*, 401-415.
8. Shuler, M.G., and Bear, M.F. (2006). Reward timing in the primary visual cortex. Science *311*, 1606-1609.
9. von Pfostl, V., Li, J., Zaldivar, D., Goense, J., Zhang, X., Serr, N., Logothetis, N.K., and Rauch, A. (2012). Effects of lactate on the early visual cortex of non-human primates, investigated by pharmaco-MRI and neurochemical analysis. NeuroImage *61*, 98-105.
10. Goense, J., Logothetis, N.K., and Merkle, H. (2010). Flexible, phase-matched, linear receive arrays for high-field MRI in monkeys. Magn Reson Imaging *28*, 1183-1191.
11. Zappe, A.C., Pfeuffer, J., Merkle, H., Logothetis, N.K., and Goense, J.B. (2008). The effect of labeling parameters on perfusion-based fMRI in nonhuman primates. J Cereb Blood Flow Metab *28*, 640-652.
12. Goense, J.B., and Logothetis, N.K. (2008). Neurophysiology of the BOLD fMRI signal in awake monkeys. Curr Biol *18*, 631-640.
13. Seamans, J.K., and Yang, C.R. (2004). The principal features and mechanisms of dopamine modulation in the prefrontal cortex. Prog Neurobiol *74*, 1-58.
14. Happel, M.F., Deliano, M., Handschuh, J., and Ohl, F.W. (2014). Dopamine-modulated recurrent corticoefferent feedback in primary sensory cortex promotes detection of behaviorally relevant stimuli. J Neurosci *34*, 1234-1247.
15. Jacob, S.N., Ott, T., and Nieder, A. (2013). Dopamine regulates two classes of primate prefrontal neurons that represent sensory signals. J Neurosci *33*, 13724-13734.
16. de Lafuente, V., and Romo, R. (2011). Dopamine neurons code subjective sensory experience and uncertainty of perceptual decisions. PNAS *108*, 19767-19771.
17. Servan-Schreiber, D., Printz, H., and Cohen, J.D. (1990). A network model of catecholamine effects: gain, signal-to-noise ratio, and behavior. Science *249*, 892-895.
18. Stanisor, L., van der Togt, C., Pennartz, C.M., and Roelfsema, P.R. (2013). A unified selection signal for attention and reward in primary visual cortex. PNAS *110*, 9136-9141.
19. Serences, J.T. (2008). Value-based modulations in human visual cortex. Neuron *60*, 1169-1181.
20. Lidow, M.S., Goldman-Rakic, P.S., Gallager, D.W., and Rakic, P. (1991). Distribution of dopaminergic receptors in the primate cerebral cortex: quantitative autoradiographic analysis using [3H]raclopride, [3H]spiperone and [3H]SCH23390. Neuroscience *40*, 657-671.
21. Gottberg, E., Montreuil, B., and Reader, T.A. (1988). Acute effects of lithium on dopaminergic responses: iontophoretic studies in the rat visual cortex. Synapse *2*, 442-449.
22. Reader, T.A. (1978). The effects of dopamine, noradrenaline and serotonin in the visual cortex of the cat. Experientia *34*, 1586-1588.

23. Phillipson, O.T., Kilpatrick, I.C., and Jones, M.W. (1987). Dopaminergic Innervation of the Primary Visual-Cortex in the Rat, and Some Correlations with Human Cortex. Brain Res Bull *18*, 621-633.
24. Tombaugh, G.C., and Somjen, G.G. (1996). Effects of extracellular pH on voltage-gated Na+, K+ and Ca2+ currents in isolated rat CA1 neurons. J Physiol *493*, 719-732.
25. Algaze, A., Leguire, L.E., Roberts, C., Ibinson, J.W., Lewis, J.R., and Rogers, G. (2005). The effects of L-dopa on the functional magnetic resonance imaging response of patients with amblyopia: a pilot study. J AAPOS *9*, 216-223.
26. Weis, T., Puschmann, S., Brechmann, A., and Thiel, C.M. (2012). Effects of L-dopa during auditory instrumental learning in humans. PloS one *7*, e52504.
27. Pleger, B., Blankenburg, F., Ruff, C.C., Driver, J., and Dolan, R.J. (2008). Reward facilitates tactile judgments and modulates hemodynamic responses in human primary somatosensory cortex. J Neurosci *28*, 8161-8168.
28. Krimer, L.S., Muly, E.C., 3rd, Williams, G.V., and Goldman-Rakic, P.S. (1998). Dopaminergic regulation of cerebral cortical microcirculation. Nature Neurosci *1*, 286-289.
29. Mandeville, J.B., Jenkins, B.G., Kosofsky, B.E., Moskowitz, M.A., Rosen, B.R., and Marota, J.J. (2001). Regional sensitivity and coupling of BOLD and CBV changes during stimulation of rat brain. Magn Reson Med *45*, 443-447.
30. Mandeville, J.B., Sander, C.Y., Jenkins, B.G., Hooker, J.M., Catana, C., Vanduffel, W., Alpert, N.M., Rosen, B.R., and Normandin, M.D. (2013). A receptor-based model for dopamine-induced fMRI signal. NeuroImage *75C*, 46-57.
31. Esaki, T., Itoh, Y., Shimoji, K., Cook, M., Jehle, J., and Sokoloff, L. (2002). Effects of dopamine receptor blockade on cerebral blood flow response to somatosensory stimulation in the unanesthetized rat. J Pharmacol Exp Ther *303*, 497-502.
32. Delfino, M., Kalisch, R., Czisch, M., Larramendy, C., Ricatti, J., Taravini, I.R., Trenkwalder, C., Murer, M.G., Auer, D.P., and Gershanik, O.S. (2007). Mapping the effects of three dopamine agonists with different dyskinetogenic potential and receptor selectivity using pharmacological functional magnetic resonance imaging. Neuropsychopharmacology : official publication of the American College of Neuropsychopharmacology *32*, 1911-1921.
33. Jenkins, B.G., Sanchez-Pernaute, R., Brownell, A.L., Chen, Y.C., and Isacson, O. (2004). Mapping dopamine function in primates using pharmacologic magnetic resonance imaging. J Neurosci *24*, 9553-9560.
34. Leonard, B.E., and Shallice, S.A. (1971). Some Neurochemical Effects of Amphetamine, Methylamphetamine and Para Bromomethyl Amphetamine in Rat. British J Pharmacol *41*, 198-&.
35. Goense, J., Merkle, H., and Logothetis, N.K. (2012). High-resolution fMRI reveals laminar differences in neurovascular coupling between positive and negative BOLD responses. Neuron *76*, 629-639.
36. Choi, J.K., Mandeville, J.B., Chen, Y.I., Grundt, P., Sarkar, S.K., Newman, A.H., and Jenkins, B.G. (2010). Imaging brain regional and cortical laminar effects of selective D3 agonists and antagonists. Psychopharmacology *212*, 59-72.
37. Choi, J.K., Chen, Y.I., Hamel, E., and Jenkins, B.G. (2006). Brain hemodynamic changes mediated by dopamine receptors: Role of the cerebral microvasculature in dopamine-mediated neurovascular coupling. NeuroImage *30*, 700-712.
38. Laughlin, S.B., de Ruyter van Steveninck, R.R., and Anderson, J.C. (1998). The metabolic cost of neural information. Nature Neurosci *1*, 36-41.
39. Porrino, L.J., Burns, R.S., Crane, A.M., Palombo, E., Kopin, I.J., and Sokoloff, L. (1987). Local cerebral metabolic effects of L-dopa therapy in 1-methyl-4-phenyl-1,2,3,6-tetrahydropyridine-induced parkinsonism in monkeys. PNAS *84*, 5995-5999.
40. Kim, S.G., and Ogawa, S. (2012). Biophysical and physiological origins of blood oxygenation level-dependent fMRI signals. J Cereb Blood Flow Metab *32*, 1188-1206.

41. Obayashi, S., Nagai, Y., Suhara, T., Okauchi, T., Inaji, M., Iriki, A., and Maeda, J. (2009). Monkey brain activity modulated by reward preferences: a positron emission tomography study. Neurosci Res *64*, 421-428.
42. Hershey, T., Black, K.J., Carl, J.L., and Perlmutter, J.S. (2000). Dopa-induced blood flow responses in nonhuman primates. Exp Neurol *166*, 342-349.
43. Leenders, K.L., Wolfson, L., Gibbs, J.M., Wise, R.J., Causon, R., Jones, T., and Legg, N.J. (1985). The effects of L-DOPA on regional cerebral blood flow and oxygen metabolism in patients with Parkinson's disease. Brain *108 (Pt 1)*, 171-191.
44. Montastruc, J.L., Celsis, P., Agniel, A., Demonet, J.F., Doyon, B., Puel, M., Marc-Vergnes, J.P., and Rascol, A. (1987). Levodopa-induced regional cerebral blood flow changes in normal volunteers and patients with Parkinson's disease. Lack of correlation with clinical or neuropsychological improvements. Mov Disord *2*, 279-289.
45. Zappe, A.C., Uludag, K., and Logothetis, N.K. (2008). Direct measurement of oxygen extraction with fMRI using 6% CO2 inhalation. Magn Reson Imaging *26*, 961-967.
46. Sicard, K.M., and Duong, T.Q. (2005). Effects of hypoxia, hyperoxia, and hypercapnia on baseline and stimulus-evoked BOLD, CBF, and CMRO2 in spontaneously breathing animals. NeuroImage *25*, 850-858.
47. Blicher, J.U., Stagg, C.J., O'Shea, J., Ostergaard, L., MacIntosh, B.J., Johansen-Berg, H., Jezzard, P., and Donahue, M.J. (2012). Visualization of altered neurovascular coupling in chronic stroke patients using multimodal functional MRI. J Cereb Blood Flow Metab *32*, 2044-2054.

FIGURE LEGENDS

Figure 1. BOLD Responses under L-DOPA+Carbidopa Influence in Visual Cortex

A. Experimental paradigm and design. The stimulus was a rotating checkerboard of 48 s followed by an isoluminant blank screen of 48 s (right panel). Every experiment was divided into three conditions: 1. a 12.8-min experiment without pharmacological manipulation; 2. a 12.8-min session with Carbidopa preconditioning (1.5 mg/kg diluted in 50 ml of PBS and injected at 1.1 ml/min); 3. a 46 min session consisting of LDC manipulation (2.1 mg/kg + 0.5 mg/kg diluted in 50 ml of PBS and injected at 1.1 ml/min over a period of 12 min). B. Activation maps showing voxels with a significant response to the visual stimulus (A09; 8-shot GE-EPI (FOV: 72x72 mm^2; TE/TR: 20/3000 ms; flip-angle 90˚; matrix: 96x96) overlaid on an anatomical scan (FLASH), acquired at 7T with an in-plane resolution of 0.75x0.75 mm^2 and 2 mm slice thickness). C. The average BOLD time course (928 volumes) over 18 fMRI experimental sessions (5 animals) shows a decrease in visually induced modulation by L-DOPA+Carbidopa; the green and the red lines show the start and stop of the L-DOPA-Carbidopa infusion. D. The average BOLD response to the visual stimulus (left) decreased by 50% compared to the pre-drug period while the baseline did not change under L-DOPA+Carbidopa (right). The shaded areas represent the SE.

Figure 2. Systemic Application of L-DOPA+Carbidopa Increases Neural Responses in V1

Average time course of the neural activity (LFP- and MUA bands) across experiments in response to L-DOPA+Carbidopa injection (n=16). A. theta band (4-8 Hz). B. gamma LFP band (40-150 Hz). C. MUA (900-3000 Hz). The green and red lines denote the beginning and end of the systemic LDC infusion. In the MUA and gamma bands, the amplitude of the visual response increased after LDC, while the variability of the baseline decreased. D. Percentage change in visual response of the gamma band (blue) and MUA (red). E. The SNR of the gamma band (blue) and the MUA (red) increased upon DA infusion. No changes were observed in the theta band. The shaded areas represent the SE.

Figure 3. Local Application of Dopamine does not alter Neural Responses in V1

Average time course of the neural activity (LFP and MUA bands) across experiments, in response to local application of DA (n=10; DA was diluted in ACSF to a final concentration of 5 mM). A. theta band (4-8 Hz). B. gamma LFP band (40-150 Hz). C. MUA (900-3000 Hz). The green and red lines denote the beginning and end of the DA infusion. In the MUA and gamma bands, the amplitude of the visual response was not affected by DA infusion. D. Percentage change in visual response of the gamma (blue) band and MUA (red). E. The SNR of the gamma band (blue) and the MUA (red) shows no changes upon DA. No changes were observed in the theta band. The shaded areas represent the SE.

Figure 4. CBF increases with L-DOPA+Carbidopa

A. Activation patterns of functional CBF (using flow sensitive alternating inversion recovery, FAIR) in early visual cortex (monkey A09) in response to visual stimulation. B. The average time course over six CBF experimental sessions shows an increase in baseline- as well as visually induced CBF (six sessions acquired at 7T: TI 1400 ms; slab 6 mm; FOV 5.5x2.4 mm^2; TE/TR 9.5/4500 ms; BW 150 kHz, and one at 4.7T: TI 1400 ms; slab 6 mm; FOV 6x3.2 mm^2; TE/TR 9.1/4500 ms; BW 125 kHz). C. The average visually induced modulation increased by 43% (left) and the baseline changed by 31% (right) upon L-DOPA+Carbidopa infusion. The shaded areas represent the SE.

Figure

Figure 1

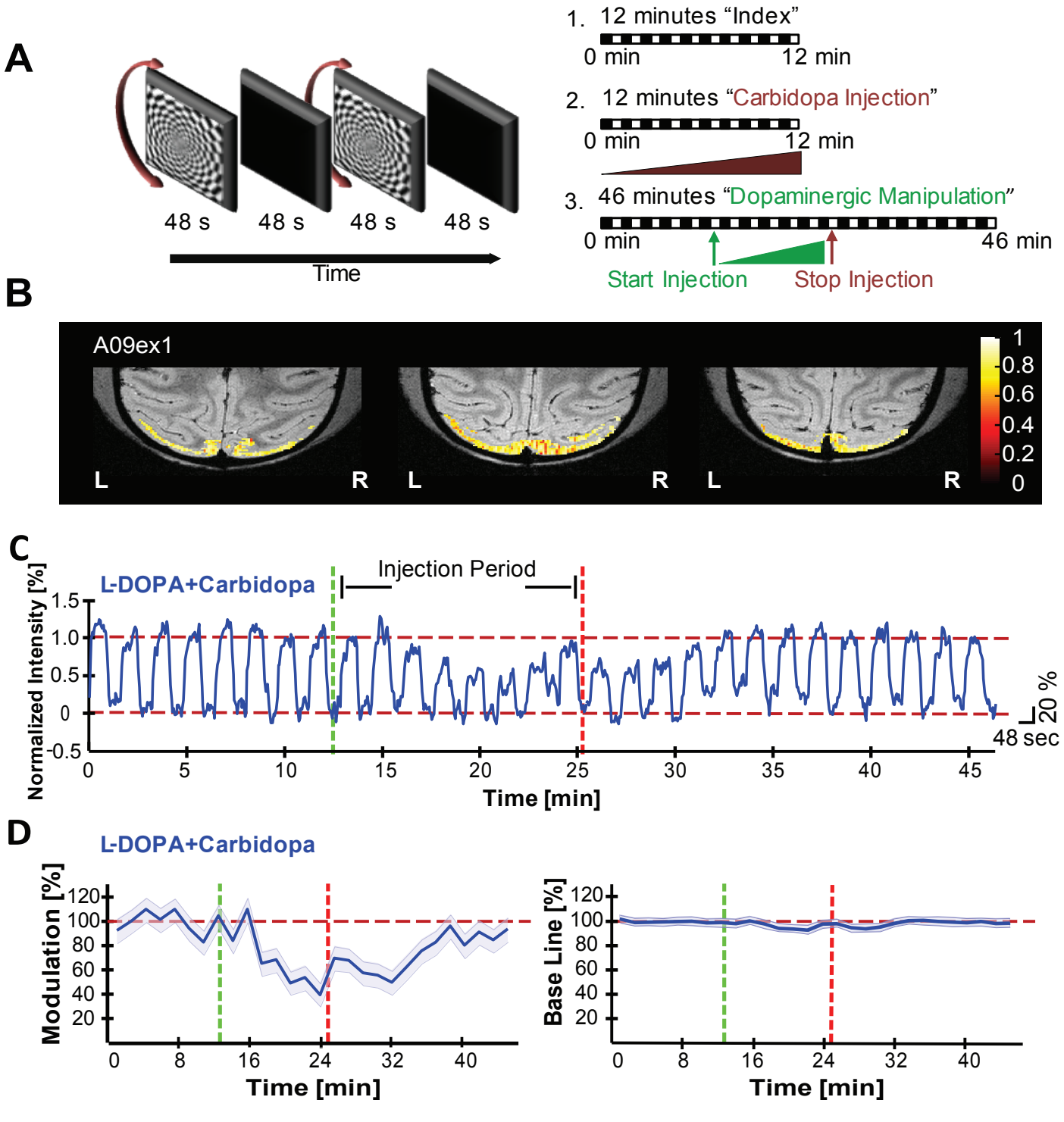

Figure

Figure 2

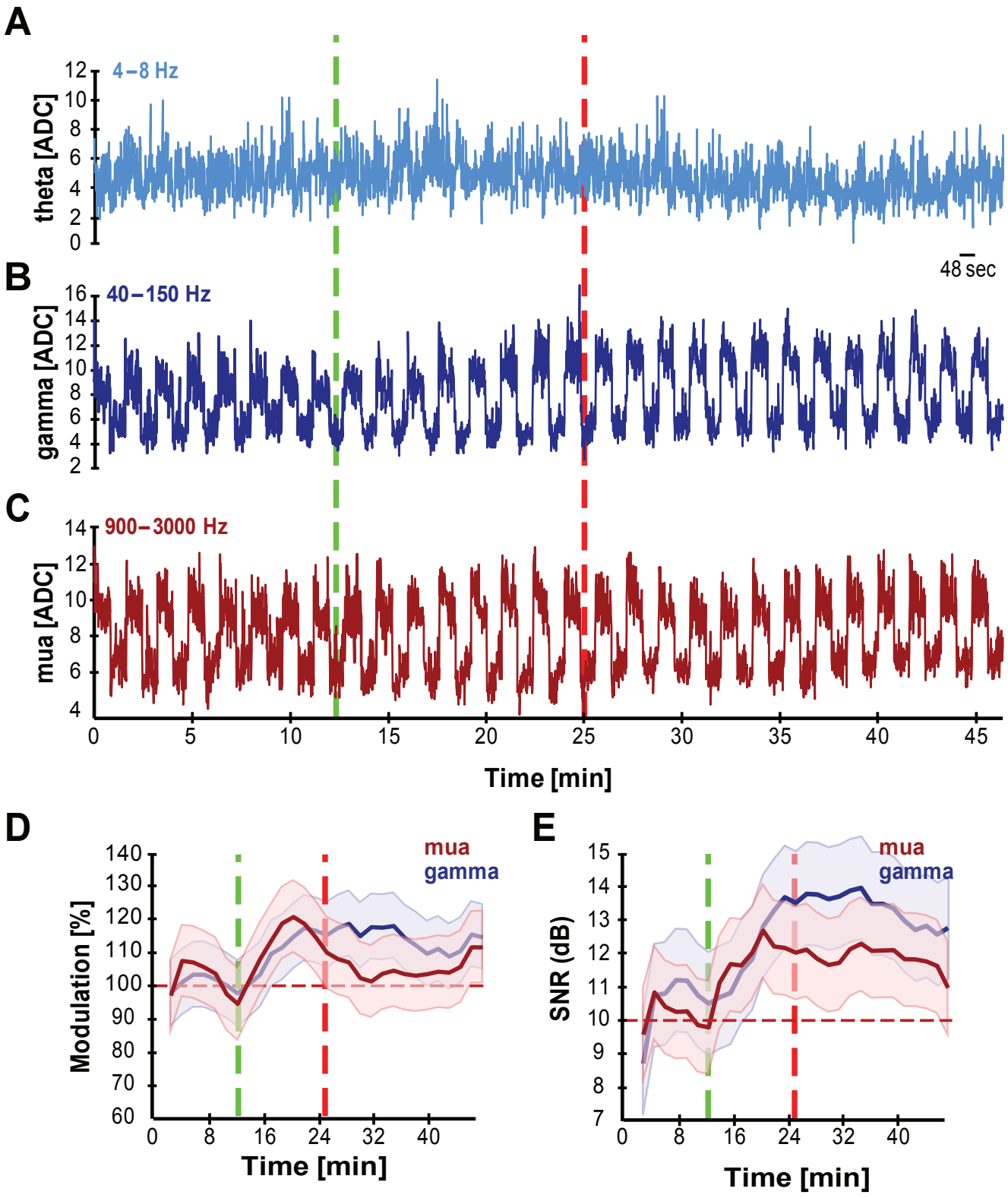

Figure

Figure 3

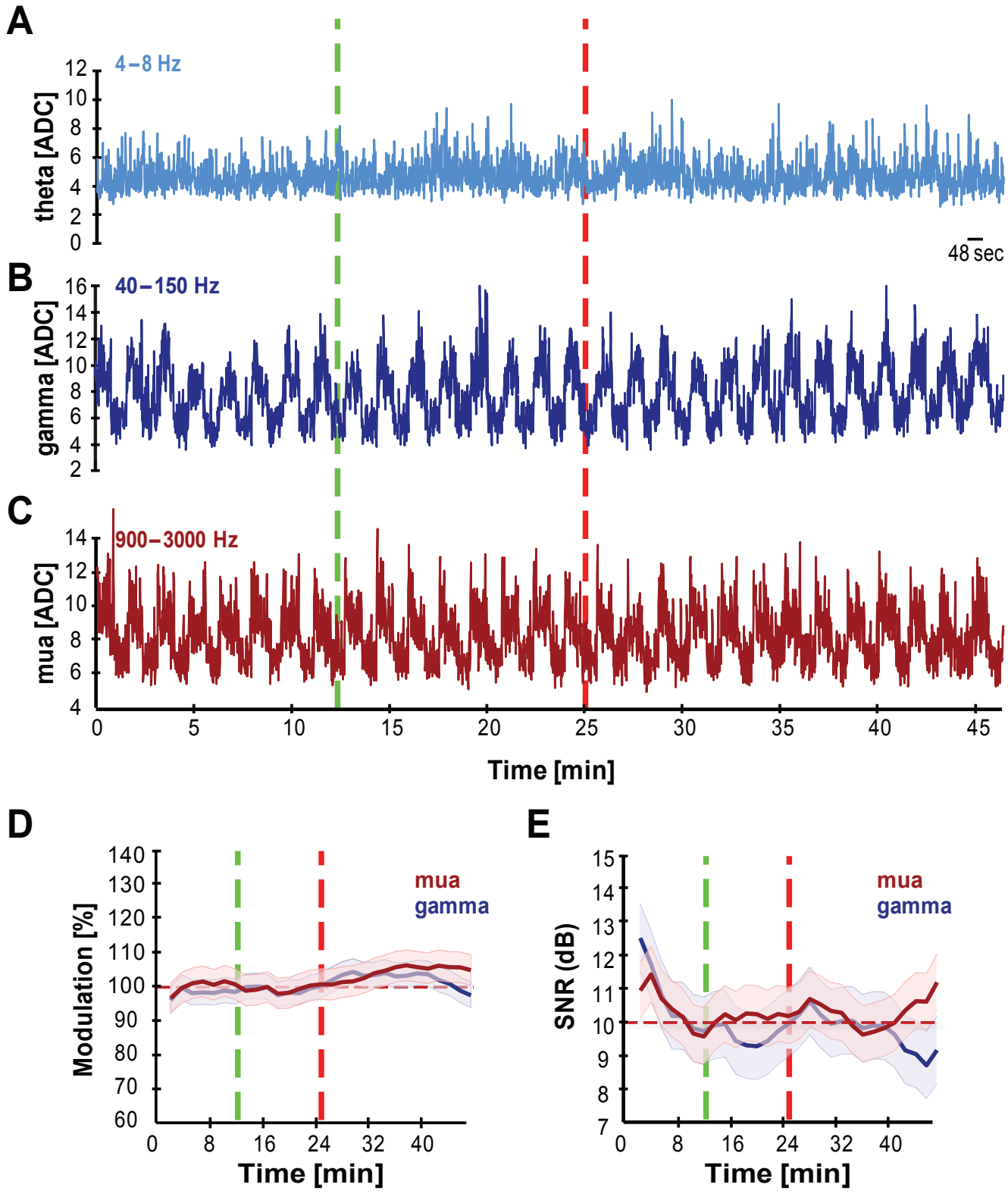

Figure

Figure 4

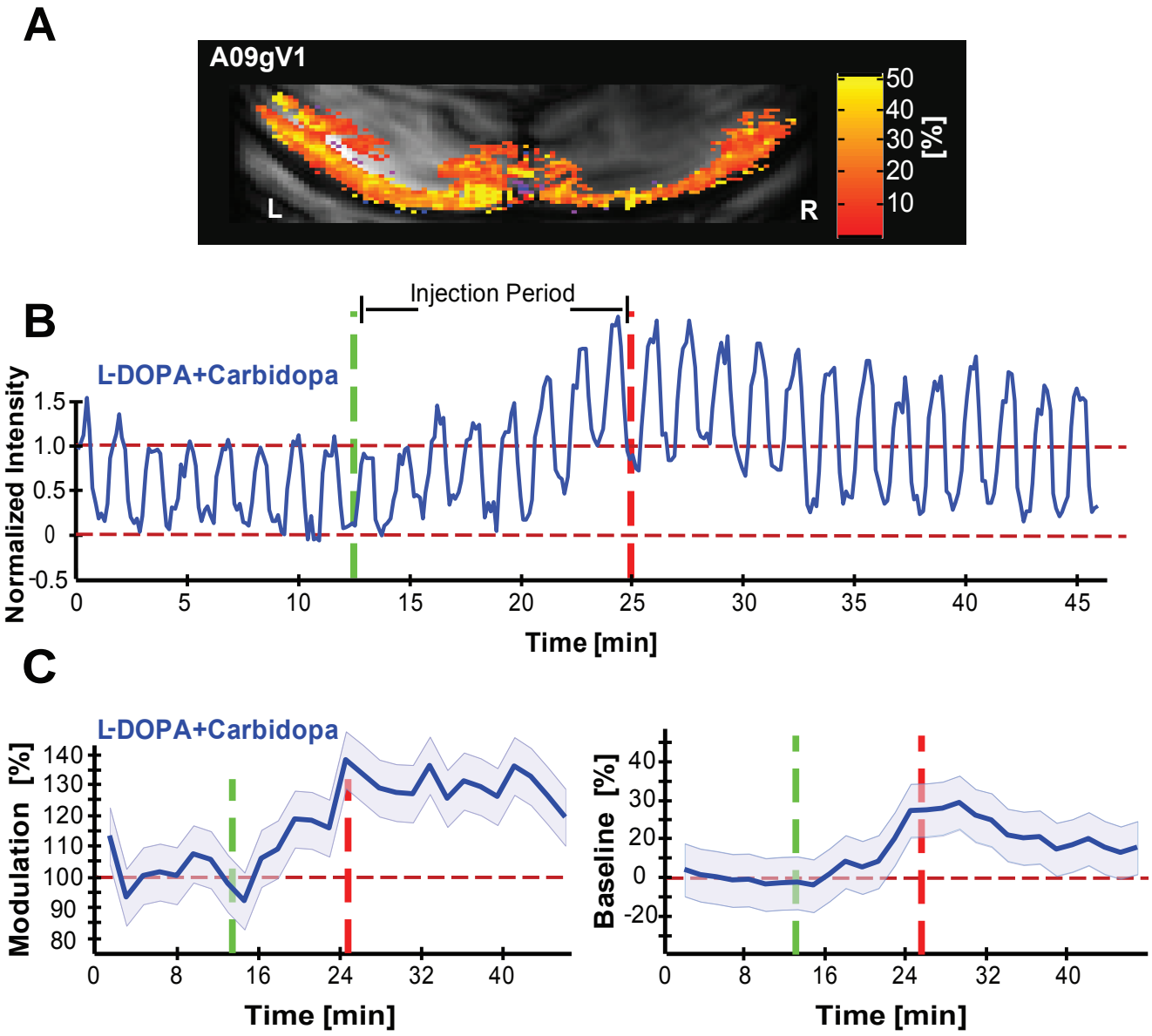

Supplemental Results

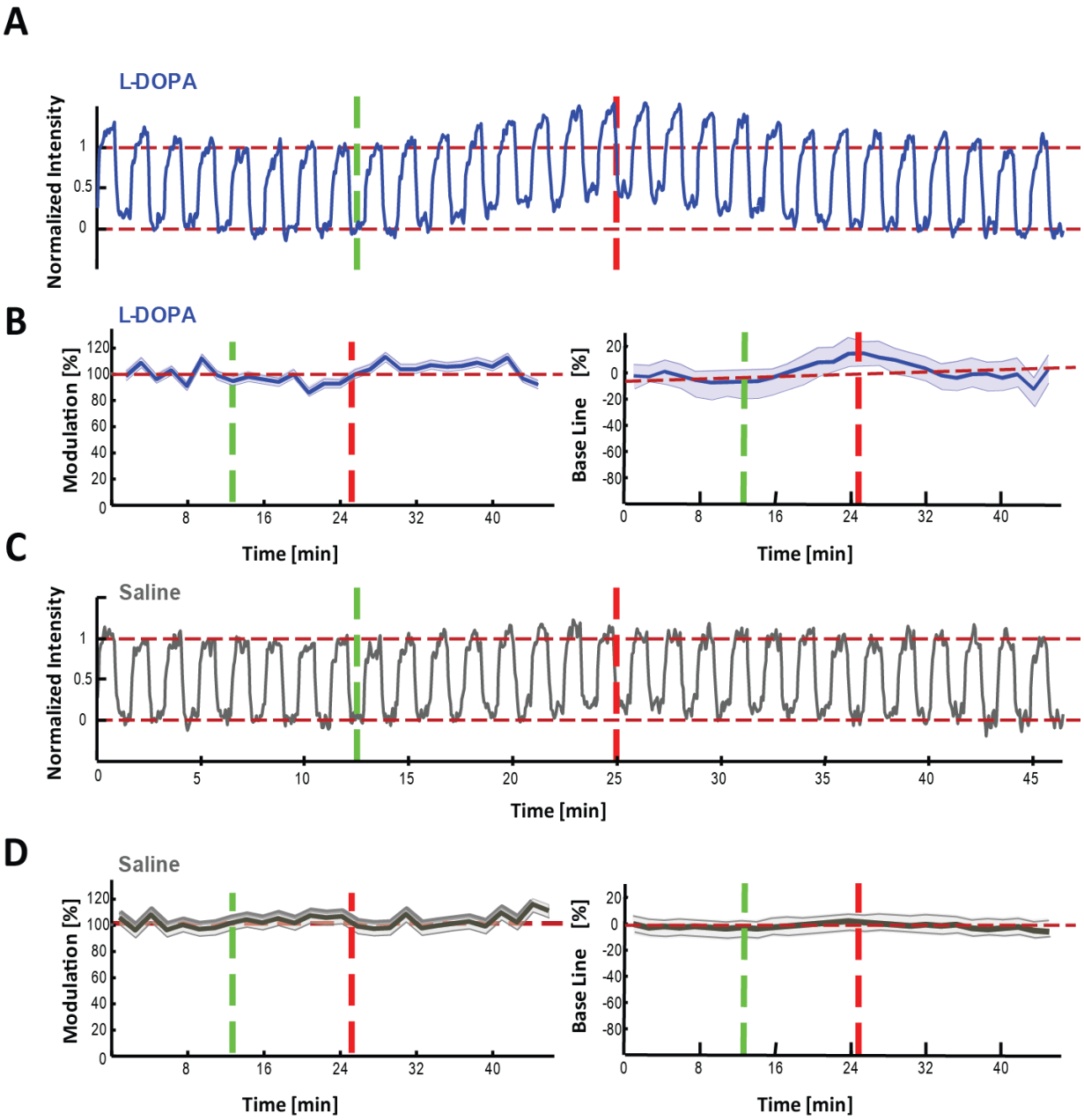

Figure S1. Effects of L-DOPA without Carbidopa and saline

A. Average BOLD time course over five fMRI experimental sessions of L-DOPA application without Carbidopa (shown in blue). The green and red lines show the start and stop of the L-DOPA infusion. B. The average visually induced modulation did not change (left) while the baseline showed a small increase (right). The systemic changes in the peripheral vascular system and the lack of effects on the visual modulation indicate the breakdown of L-DOPA in the periphery. C. Shows the average BOLD time course during saline infusion, similarly green and red lines denote the infusion period (shown in gray). D. Visually induced modulation (left) and baseline (right) did not change in response to saline infusion.

L-DOPA without Carbidopa intervention and saline control

Systemic L-DOPA, without any Carbidopa was applied in three animals. Concentrations, flow and final volume were similar to those used in the L-DOPA+Carbidopa interventions. Figure S1A shows the averaged BOLD responses across all experimental sessions (n = 5, upper panel, blue). As in the L-DOPA+Carbidopa condition we divided each session in three conditions: 'pre-drug', 'drug' and 'post-drug' and calculated the changes in the visually induced modulation and in the baseline. There were no changes in the visually induced modulation during (MOD_{drug} = 99%; p = 0.09 paired t-test;) and after the injection (MOD_{post} = 104%; p = 0.09 paired t-test; $median_{post}$ = 101%). We observed a significant increase in the baseline BOLD signal during and after the injection period (Figure S1B). The increase was evident ~8 min after the start of the injection ($BOLD_{baseline,drug}$ = 112 ± 8%; p = 0.05 paired t-test; median $BOLD_{baseline,drug}$ = 108%). This increase lasted ~10 min after the injection was stopped ($BOLD_{post,drug}$ = 116 ± 6%; p = 0.05 paired-test; median $BOLD_{post,drug}$ = 112%). Systemic injection of saline showed that both the visually induced modulation and the baseline were unchanged during and after injection (Figure S1C,D; MOD_{drug} = 102%; $median_{drug}$ = 107%; p = 0.08 paired t-test; MOD_{post} = 104%; $median_{post}$ = 102%; p = 0.23 paired t-test).

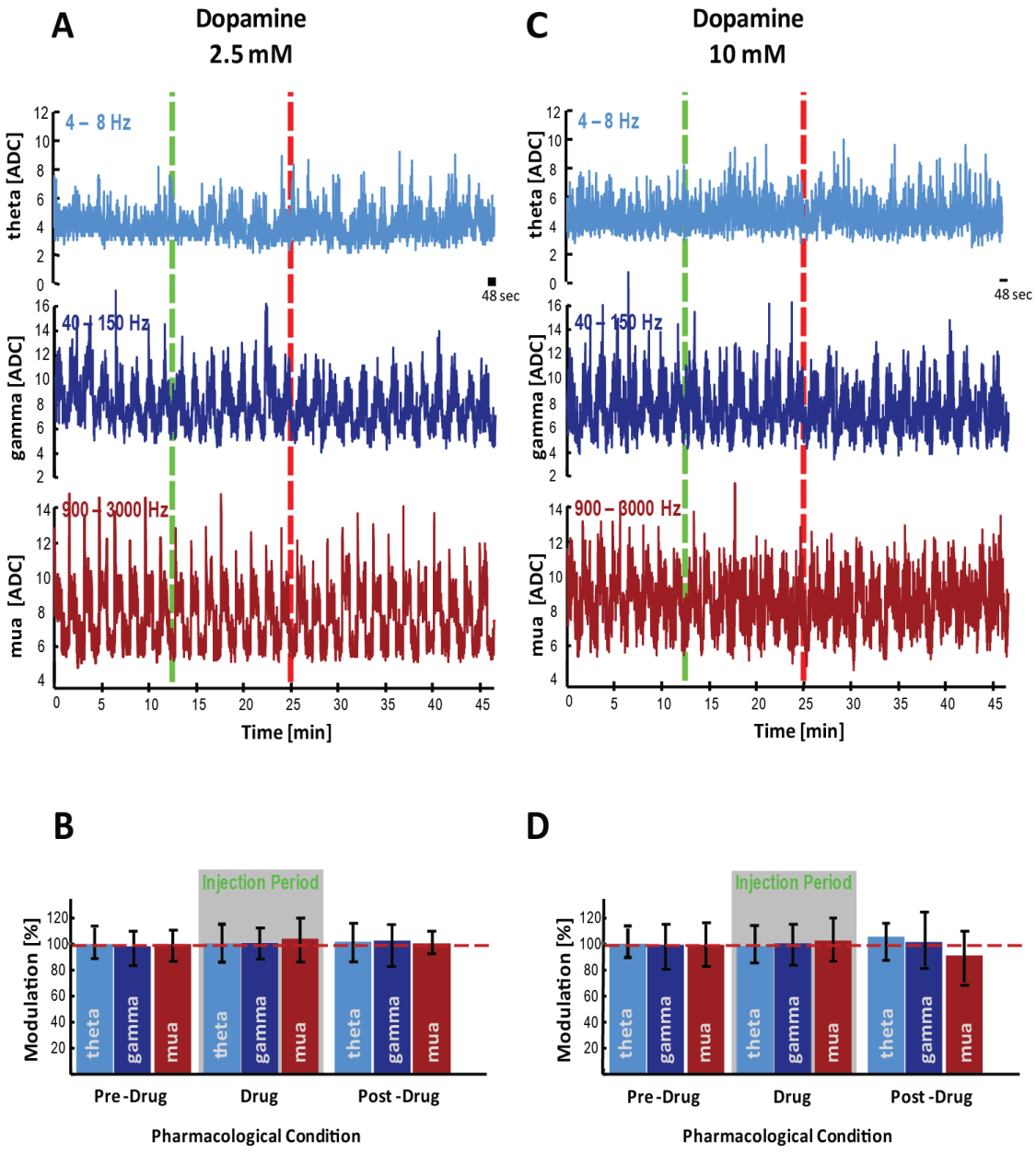

Figure S2. V1 responses to local DA application at different concentrations.

Average time courses of the neural activity (LFP and MUA bands) across experiments, in response to local application of DA at different concentrations. A. DA at 2.5 mM: responses in θ-band (4-8 Hz), γ-band (40-150 Hz) and MUA (900-3000 Hz). The green and red lines denote the beginning and end of the DA infusion. B. Changes in visually induced modulation for each of the bands recorded during the pre-drug, drug, post-drug condition; no changes were observed at this concentration. C. DA at 10 mM: responses in θ-band, γ-band and MUA. D. No changes in visually induced modulation were observed upon dopamine application.

Effect of different concentrations of dopamine in V1

We locally applied dopamine at different concentrations in V1 (2.5 and 10 mM; Figure S2). Figure S2A and S2B show the results for the 2.5 mM condition. Figure S2C and S2D show the 10 mM condition. Both pharmacological conditions were divided in pre-drug, drug and post-drug, for which we calculated the PSD for the θ (4-8 Hz), γ (40-150 Hz) and MUA- (900-3000 Hz) bands. No significant effects were observed in any of the computed frequency bands for both pharmacological manipulations.

Animal	Heart Rate (pulse/min)			Blood Pressure (mm/Hg)			CO_2			SpO_2		
	Pre	Drug	Post	Pre	Drug	Post	Pre	Drug	Post	Pre	Drug	Post
A09	127±12	131±8	129±9	91/38	96/40	92/35	32±2	33±1	33±2	98	99	99
G09	123±9	112±15	112±12	109/53	111/47	112/47	33±2	33±1	33±2	100	99	990
H09	130±8	125±2	128±15	110/48	113/44	121/38	33±1	33±1	32±2	98	100	100
H11	110±12	114±7	120±12	152/56	152/54	149/51	33±1	32±1	33±2	99	99	98
K07	103±6	106±8	106±11	86/35	75/29	72/30	33±1	33±1	33±2	98	99	99
J08	108±4	101±12	102±14	78/43	74/39	85/29	32±1	33±1	33±1	98	100	99

Table 1. Mean physiological parameters under general anesthesia

Included in the table are the mean physiological parameters under general anesthesia during the pre-drug, drug and post-drug conditions (four females and two males). The parameters included in this table were computed across all experimental sessions.

Supplemental Experimental Procedures

Anesthesia and visual stimulation for neurophysiology and fMRI experiments

The anesthesia protocol has been described previously **[1, 2]**. Briefly, glycopyrrolate (0.01 $mg \cdot kg^{-1}$) and ketamine (15 $mg \cdot kg^{-1}$) were used for preanesthesia. After induction with fentanyl (3 $mg \cdot kg^{-1}$), thiopental (5 $mg \cdot kg^{-1}$) and succinylcholine chloride (3 $mg \cdot kg^{-1}$), animals were intubated and ventilated using a Servo Ventilator 900C (Siemens, Germany) maintaining an end-tidal CO_2 of 33-35 mm Hg and oxygen saturation above 95%. The anesthesia was maintained with remifentanil (0.4 – 1 $\mu g \cdot kg^{-1} min$) and mivacurium chloride (2 – 6 $mg \cdot kg^{-1} h$) to ensure complete paralysis of the eye muscles. In our previous work on neurovascular coupling in V1 we showed that neural responses and neurovascular coupling under this anesthesia regimen are very similar to those in the awake state **[2, 3]**. In a comparison of (face-selective) visual responses between awake and anesthetized monkeys **[4]** few differences in the activated areas were seen throughout the brain. Furthermore, μ-opioid receptors are located at high densities in basal ganglia and thalamus, especially in regions associated to motor commands, but regions associated with cognition, ventral tegmental area, substantia nigra and frontal regions, have low densities of μ-opioid receptors. Therefore, we expect that the anesthesia used, does not cause major interference with DAergic effects on neural responses and neurovascular coupling.

fMRI signals are very sensitive to changes in body temperature, pH, blood pressure and oxygenation, the physiological state of the monkey was monitored continuously and kept within normal limits. Body temperature was tightly maintained at 38.5-39.5°C. Throughout the experiment lactate Ringer's (Jonosteril, Fresenius Kabi, Germany) with 2.5% glucose was continuously infused at a rate of 10 $ml \cdot kg^{-1} \cdot hr^{-1}$ to maintain an adequate acid-base balance and intravascular volume and blood pressure; hydroxyethyl starch (Volulyte, Fresenius Kabi, Germany) was administered as needed.

Two drops of 1% cyclopentolate hydrochloride were used in each eye to achieve mydriasis. The visual stimuli were presented binocularly using a custom-made MR-compatible display system with a resolution of 800 x 600 pixels and a frame rate of 60 Hz. Animals were wearing hard contact lenses (Wöhlk-Contact-Linsen, Schönkirchen, Germany) to focus the eyes on the stimulus plane. The eyepieces of the stimulus presentation system were positioned using a modified fundus camera **[**Zeiss RC250; see **1]**). The visual stimulation protocol consisted of blocks of rotating black and white polar checkerboards of 10x10° in size lasting 48 seconds alternated with an isoluminant gray blank period of equal length. The stimulus timing was controlled by a computer running a real-time OS (QNX, Ottawa, Canada). The direction of the rotation was reversed every 8 s to minimize adaptation. This block was repeated 29 times yielding in total 46 minutes for each experiment.

Systemic and Local Injections

Systemic applications of L-DOPA+Carbidopa and saline were performed with a custom-made pressure-operated pump **[5]**. The actual flow and volume were continuously monitored by high precision flow-meters (Sensirion, Switzerland). The preconditioning with Carbidopa consisted of 1.5 mg/kg diluted in 50 ml and injected at 1.1 ml/min over a period of 12 minutes. The combined L-DOPA+Carbidopa applications consisted of a total amount of 2.1 mg/kg + 0.5 mg/kg, diluted in 50 ml injected at 1.1 ml/min over 12 min. All the drugs that were systemically applied were diluted in a phosphate-buffered-saline (PBS) solution and the pH was adjusted with NaOH to 7.35. The PBS solution was composed of NaCl 137 mM, KCl 2.7 mM, Na_2HPO_4 8.1 mM, KH_2PO_4 1.76 mM. The control experiments were performed with the PBS solution where we applied the same volume at similar flow rate (5 experimental sessions). Because of the sensitivity of the BOLD and CBF measurements, injections were done over a period of 12 min to avoid changes in blood volume or volume-related changes in other physiological parameters, and no adjustments to the anesthesia were made during the 46-min scan.

Local applications of DA in V1 were performed using three independent injection lines driven by three separate HPLC pumps (M5, VICI, USA) **[6]**. The three independent lines allowed us to switch between different solutions in successive trials within one experiment. All lines were monitored by high-precision flow meters (Sensirion, Switzerland) controlling the exact applied volume and flow. The DA-containing solution was freshly prepared using DA-hydrochloride diluted in artificial cerebrospinal fluid (ACSF) at final concentrations of 2.5-10 mM. The pH was adjusted to 7.35 with NaOH. The ASCF consisted of NaCl 148.19 mM, KCl 3.0 mM, $CaCl_2$ 1.40 mM, $MgCl_2$ 0.80 mM, Na_2HPO_4 0.20 mM. The control solution was the unmodified ACSF solution. All chemicals for local and systemic application were purchased from Sigma Aldrich (Schnelldorf, Germany). ACSF and DA injections were delivered at 0.6 µl/min for a duration of 12 min.

Data analysis procedures were implemented using custom-written routines in MatLab (Mathworks, Natick, MA). No smoothing was applied in any of the data sets. The electrophysiology and fMRI (BOLD and CBF) scans were divided in three epochs: the 'pre-drug', 'drug' and 'post-drug' periods. The 'pre-drug' period consisted of 8 blocks of visual stimulation (12.8 min) while the 'drug' condition consisted of systemic (L-DOPA+Carbidopa or PBS) or local (DA or ACSF) infusion starting immediately after 8 blocks of visual stimulation. We used the 'pre-drug' period as a reference to compute changes during the 'drug' and 'post-drug' periods, from the visual induced modulation, baseline and the SNR of the electrophysiology signals. Statistical significance in all the data was accessed by using a paired t-test comparing the 'pre-drug' period with the 'drug' and 'post-drug' period. This procedure was performed for the statistical significance in changes of the visual-induced modulation, baseline changes and SNR.

Neurophysiology data collection and analysis

For electrophysiological recordings first a small skull trepanation (~3 mm diameter) was made. Subsequently, the meninges were visualized with a microscope (Zeiss Opmi

MDU/S5, Germany) and carefully dissected. Electrodes were NeuroNexus laminar probes (NeuroNexus Technologies, Ann Arbor, USA) for all recordings. We used a 16-contact probe on a single shank of 3 mm length and 50 µm thickness. The electrode sites were spaced 100 µm apart, with a recording area of 413 μm^2. The impedance of the contact points ranged from 500 to 700 kΩ. The electrodes were slowly advanced into the visual area under visual and auditory guidance using a manual micromanipulator (Narashige Group, Japan). The depth was determined based on the spontaneous spiking activity of each of the cortical layers **[7]**. The signals were amplified and filtered into a band of 1 Hz – 8 kHz (Alpha-Omega Engineering, Nazareth, Israel) and digitized at 20.833 kHz with 16-bit resolution (National Instruments, Austin, TX), ensuring sufficient resolution for both local field potentials and spiking activity. The recording area was filled with a mixture of 0.6% agar dissolved in NaCl 0.9%, pH 7.4 which guaranteed a good electrical connection between the ground contact and the animal **[8]**.

To analyze electrophysiology data, we used a one-second window to calculate the power spectral density in three frequency bands: low LFP (θ: 4-8 Hz), high LFP (γ: 40-150 Hz) and MUA (900-3000 Hz) **[9]**. The θ-band was used to indicate whether LDC affects the broadband LFP power and to assess whether DA-injection induces changes in the level of anesthesia **[10]**. The signal-to-noise ratio (SNR) of the electrophysiological signals was calculated by dividing the power of the visually evoked responses (meaningful information) by the power of the responses during the off-period.

MRI data collection and analysis

The fMRI experiments were conducted in a vertical 7T scanner with a 60 cm diameter bore (Bruker BioSpin GmbH, Ettlingen, Germany) and in a vertical 4.7T with a 40 cm diameter bore. We performed fifteen BOLD experiments and five CBF experiments at 7T, and one CBF experiment at 4.7T. We used a custom-made chair to position the monkey into the magnet. For BOLD experiments, we used a custom-built quadrature volume coil that allows

imaging of deep brain structures while still maintaining a high signal-to-noise ratio in the visual cortex. We used a single-shot gradient-echo EPI with a FOV of 72x72 mm^2 and matrix size of 96x96. 11 slices were acquired with a thickness of 2 mm, TE/TR 20/3000 ms and flip angle of 90˚. Each experimental session consisted of 928 volumes. Shimming was done with FASTMAP over a volume of 12 mm^3. Six functional CBF measurements were acquired at 7T and one at 4.7T. For the CBF experiments we used a volume coil to transmit in combination with a custom-built, 4-channel phased array **[11]**. Perfusion imaging was performed using flow-sensitive alternating inversion recovery **[**FAIR; **12]**, with alternating slab-selective and nonselective inversion pulses. At 7T we used inversion time 1400 ms, slab 6 mm, FOV 5.5x2.4 mm^2, TE/TR 9.5/4500 ms and receiver BW 150 kHz. The experiments at 4.7T were performed using an inversion time 1400 ms, slab 6 mm, FOV 6x3.2 mm^2, TE/TR 9.1/4500 ms and BW 125 kHz.

We included 15 of 18 data sessions during L-DOPA injections in the data analysis; the rest were devoted to the development of the injection technique. We defined a region of interest (ROI) consisting of early visual cortex (V1-V2). A short scan (12 min) preceding the injection scan was used to define the ROI that was subsequently used for the injection scan. We used a boxcar convolved with a haemodynamic response function (gamma variant function) as regressor to calculate the correlation coefficient. Voxels showing robust visually induced modulation ($p < 0.02$) were included for further analysis, and were then monitored during the long (46.4 min) injection scan to study L-DOPA induced effects. This approach allowed us to investigate L-DOPA induced effects without making a priori assumptions.

BOLD and CBF time courses were linearly detrended and normalized. Every trace was tested for L-DOPA induced changes in the visually induced modulation. For the calculation of the modulation we subtracted the ON periods from the OFF periods, the result was then divided by the OFF period and multiplied by 100. Baseline changes were computed by taking the image intensity in the periods without visual stimulation (OFF periods). To determine how LDC affected evoked BOLD- and CBF-responses, we analyzed the

modulation in response to visual stimulation normalized to the pre-drug condition. The BOLD-modulation in the pre-drug period was 2.5±1.1%, which is typical for anesthetized monkeys at 7T **[5, 11, 13]**. Similarly, baseline changes induced by LDC were calculated by computing OFF periods normalized to the pre-drug condition **[5]**.

Supplemental References

1. Logothetis, N.K., Guggenberger, H., Peled, S., and Pauls, J. (1999). Functional imaging of the monkey brain. Nat Neurosci *2*, 555-562.
2. Logothetis, N.K., Pauls, J., Augath, M., Trinath, T., and Oeltermann, A. (2001). Neurophysiological investigation of the basis of the fMRI signal. Nature *412*, 150-157.
3. Goense, J.B., and Logothetis, N.K. (2008). Neurophysiology of the BOLD fMRI signal in awake monkeys. Curr Biol *18*, 631-640.
4. Ku, S.P., Tolias, A.S., Logothetis, N.K., and Goense, J. (2011). fMRI of the face-processing network in the ventral temporal lobe of awake and anesthetized macaques. Neuron *70*, 352-362.
5. von Pfostl, V., Li, J., Zaldivar, D., Goense, J., Zhang, X., Serr, N., Logothetis, N.K., and Rauch, A. (2012). Effects of lactate on the early visual cortex of non-human primates, investigated by pharmaco-MRI and neurochemical analysis. NeuroImage *61*, 98-105.
6. Rauch, A., Rainer, G., and Logothetis, N.K. (2008). The effect of a serotonin-induced dissociation between spiking and perisynaptic activity on BOLD functional MRI. PNAS *105*, 6759-6764.
7. Self, M.W., van Kerkoerle, T., Super, H., and Roelfsema, P.R. (2013). Distinct roles of the cortical layers of area V1 in figure-ground segregation. Curr Biol *23*, 2121-2129.
8. Oeltermann, A., Augath, M.A., and Logothetis, N.K. (2007). Simultaneous recording of neuronal signals and functional NMR imaging. Magn Reson Imaging *25*, 760-774.
9. Belitski, A., Gretton, A., Magri, C., Murayama, Y., Montemurro, M.A., Logothetis, N.K., and Panzeri, S. (2008). Low-frequency local field potentials and spikes in primary visual cortex convey independent visual information. J Neurosci *28*, 5696-5709.
10. Kortelainen, J., Vayrynen, E., and Seppanen, T. (2011). Depth of anesthesia during multidrug infusion: separating the effects of propofol and remifentanil using the spectral features of EEG. IEEE Trans Biomed Eng *58*, 1216-1223.
11. Goense, J., Logothetis, N.K., and Merkle, H. (2010). Flexible, phase-matched, linear receive arrays for high-field MRI in monkeys. Magn Reson Imaging *28*, 1183-1191.
12. Kim, S.G. (1995). Quantification of relative cerebral blood flow change by flow-sensitive alternating inversion recovery (FAIR) technique: application to functional mapping. Magn Reson Med *34*, 293-301.
13. Zappe, A.C., Pfeuffer, J., Merkle, H., Logothetis, N.K., and Goense, J.B. (2008). The effect of labeling parameters on perfusion-based fMRI in nonhuman primates. J Cereb Blood Flow Metab *28*, 640-652.